



OPEN ACCESS

EDITED BY

Ayman Elbaz,
King Abdullah University of Science and
Technology, Saudi Arabia

REVIEWED BY

Obed Majeed Ali,
Northern Technical University (NTU), Iraq
Samet Uslu,
Karabük University, Türkiye

*CORRESPONDENCE

Naushad Ahmad Ansari,
✉ naushad.nsr@gmail.com

SPECIALTY SECTION

This article was submitted to
Engine and Automotive Engineering,
a section of the journal
Frontiers in Mechanical Engineering

RECEIVED 20 September 2022

ACCEPTED 16 January 2023

PUBLISHED 30 January 2023

CITATION

Kumar M, Gautam R and Ansari NA (2023),
Performance characteristics optimization
of CRDI engine fuelled with a blend of
sesame oil methyl ester and diesel fuel
using response surface
methodology approach.
Front. Mech. Eng 9:1049571.
doi: 10.3389/fmech.2023.1049571

COPYRIGHT

© 2023 Kumar, Gautam and Ansari. This is
an open-access article distributed under
the terms of the [Creative Commons
Attribution License \(CC BY\)](https://creativecommons.org/licenses/by/4.0/). The use,
distribution or reproduction in other
forums is permitted, provided the original
author(s) and the copyright owner(s) are
credited and that the original publication in
this journal is cited, in accordance with
accepted academic practice. No use,
distribution or reproduction is permitted
which does not comply with these terms.

Performance characteristics optimization of CRDI engine fuelled with a blend of sesame oil methyl ester and diesel fuel using response surface methodology approach

Manish Kumar, Raghvendra Gautam and Naushad Ahmad Ansari*

Department of Mechanical Engineering, Delhi Technological University, Delhi, India

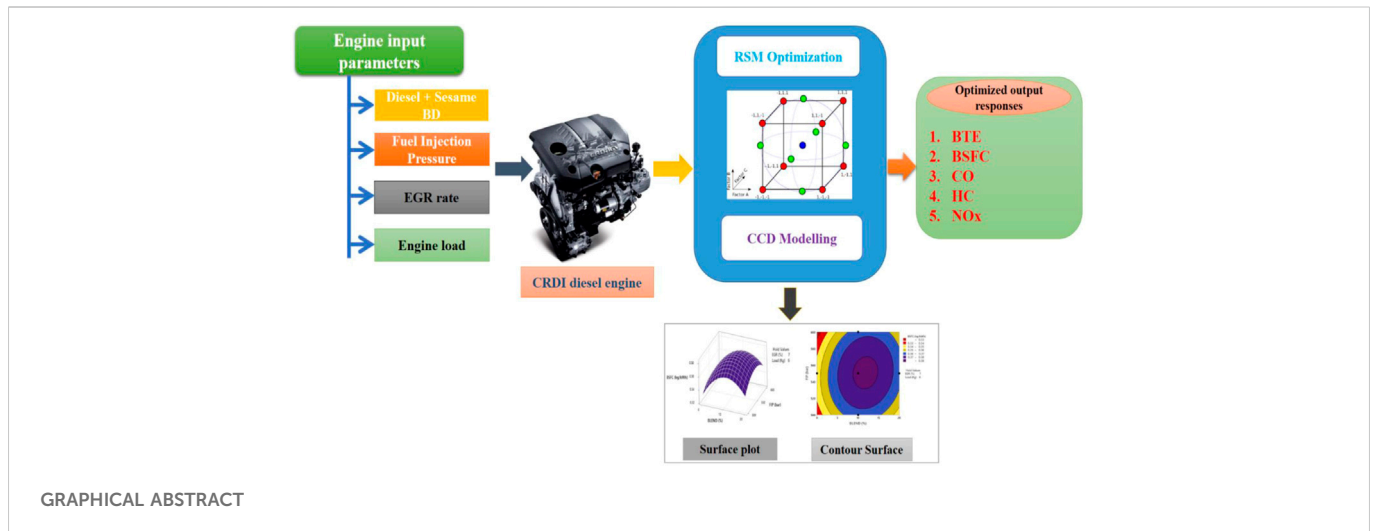
The primary aim of this experiment was to use response surface methodology (RSM) to optimize engine operating parameters for optimal performance and emission characteristics of a common rail direct injection (CRDI) diesel engine fuelled with sesame oil methyl ester (SOME)/diesel blends. The experiments were carried out on a water-cooled common rail direct injection engine with a 4-stroke, single-cylinder connected to an eddy current dynamometer. As input variables, the SOME% (0%–20%), fuel injection pressure (FIP) (500–600 bar), EGR rates (0%–14%), and engine load (0–12 kg) were used. The optimization method is utilized to maximize brake thermal efficiency (BTE) while minimizing BSFC, CO, HC, and NO_x emissions. Experimental research data were used to create the RSM model through DoE (Design of experiments). The most relevant factors impacting the responses were identified using an ANOVA analysis. According to the optimization findings, the engine's optimum working parameters were found to be a 20% SOME ratio, 577.5 bar FIP, 5.26% EGR rates, and 5.12 kg engine load. Under these operating circumstances, the optimal responses were determined to be 18.92% BTE, 0.3705 kg/kWh BSFC, 0.03190% vol. CO, 13 ppm HC, and 447.5 ppm NO_x emission. At the same time, R^2 values were 96.35%, 87.54%, 91.57%, 95.87%, and 93.73% for BTE, BSFC, CO, HC, and NO_x respectively.

KEYWORDS

sesame oil methyl ester, common rail direct injection (CRDI,), response surface methodology—RSM, emissions, performance

Highlights

- CRDI engine characteristics study on sesame oil biodiesel blend with diesel.
- Development of RSM regression and optimization model.
- The engine's optimum working parameters were found to be a 20% SOME ratio, 577.5 bar FIP, 5.26% EGR rates, and 5.12 kg engine load.
- The optimal responses were determined to be 18.92% BTE, 0.3705 kg/kWh BSFC, 0.03190% vol. CO, 13 ppm HC, and 447.5 ppm NO_x emission.
- The R^2 values were 96.35%, 87.54%, 91.57%, 95.87%, and 93.73% for BTE, BSFC, CO, HC, and NO_x respectively.



1 Introduction

The whole world's worries about energy insecurity along with the constant demands of meeting ever-stricter emission regulations have shifted the focus of the fuel business away from fossil-based fuels and toward innovative and renewable fuel sources for IC engine applications (Pali et al., 2021). Biodiesel impresses the attention of scientists and researchers in this area. These fuels are becoming increasingly appealing in the present global energy situation since they are renewable and biodegradable, as well as offering energy security and foreign exchange savings while also addressing environmental issues (Oni and Oluwatosin, 2020; Devaraj et al., 2021; Yadav and Gautam, 2022).

Biodiesel refers to a class of compounds known as alkyl esters of fatty acids, which are produced from vegetable oils or animal fats when treated with alcohol (Ganesan et al., 2021). The thermos-physical properties of biodiesel are similar to conventional diesel fuel. As a result, it may be utilised as a fuel for diesel engines without requiring any design or equipment adjustments (Bhan et al., 2022). In comparison to fossil diesel, biodiesel has a higher cetane number (CN), oxygenated, sulphur-free and lower aromatic content, which varies depending on the processing procedure and feedstock (Yesilyurt, 2020; Aljaafari et al., 2022). Several studies have found that using biodiesel as a fuel in diesel engines reduces hazardous exhaust emissions while maintaining engine performance that is comparable to diesel fuel (Rathore et al., 2019; Sayyed et al., 2022; Seeniappan et al., 2022). Hydrocarbon (HC), carbon monoxide (CO), and smoke opacity emissions were reduced in some tests, while NOx emissions rose with biodiesel fuels (Nanthagopal et al., 2020). Despite its many benefits over diesel fuel, it has several drawbacks such as low calorific value, poor cold flow characteristics, higher viscosity, oxidative stability, and maybe increased nitrogen oxides (NOx) emissions (Govindasamy et al., 2019). P Shrivastava et al. (2019) carried out experimental studies on a diesel engine powered by various biodiesel blends of Karanja and Roselle with diesel fuel and found reductions in BTE, EGT, indicated thermal efficiency, maximum rate of pressure rise rate, ID, NOx emission, and smoke levels of 4.3%, 1.2%, 0.71%, 4.93%, 2.47%, 6.01%, and 12.59% for LA20 (20% Roselle + 80% diesel) compared to diesel, and an improvement in BSFC 6.84% and CO₂ emission by 3.74%. BTE, EGT, NOx, and smoke emissions

were lowered by 1.82, 1.64, 3.83, and 13.63%, respectively, with the KB20 (20% Karanja + 80% diesel) while BSFC increased by 8.5%. Singh and Verma (2019) studied the impact of *Momordica charantia* (L.) seeds on a diesel engine mixed with conventional diesel as an alternative to biodiesel (20%). The experiment was carried out at varied engine loads and speeds. The results indicated that a 20% biodiesel mix significantly reduced NOx emissions (51.68%, 55.88%, and 55.68% at 1,200, 1,400, and 1,800 rpm), but other emission components such as CO, CO₂, PM, and SO₂ were comparable to diesel. The performance and combustion parameters were found to be inferior to those of diesel.

Sesame oil is used to make biodiesel in the current study. The sesame plant is grown in tropical to temperate climates. Sesame oil is produced in large quantities in India (25% of world production). Seeds of sesame include about 50% oil contents, as opposed to 20% oil found in soybeans. Sesame oil, contains 47% oleic acid, 39% linoleic acid, 4% stearic acid, and 10% palmitic acid. Sesame seeds are planted in May and June and grow for about a year. The growing season is from July through August, with harvesting taking place in September–November (Mehra and Pant, 2021; Mujtaba et al., 2021). These biofuels demand a greater fuel injection pressure (FIP) due to their higher viscosity, however, the injection pressure is limited in diesel engines. These issues can be resolved by introducing a CRDI system, which can inject fuel at any crank angle or injection pressure. With enhanced FIP, the process of mixing fuel droplets with air enhances due to the higher charge temperature accessible under high load circumstances (Pavan et al., 2021). To overcome the NOx emission, exhaust gas recirculation (EGR) is used which is a dependable and cost-effective technique for decreasing NOx emissions in diesel engines (Ramachander and Gugulothu, 2022). Since the 1990s, it has been widely used in automobile and heavy-duty diesel engines. EGR is an exhaust control technology that uses a control valve and input manifold to allow a part of the exhaust flow inside the cylinder. By recirculating exhaust gases into the engine's cylinder, a portion of fresh air is replaced by exhaust gas. This technique decreases the combustion temperature, which lowers the quantity of NOx produced, also lowers the gas pressure inside the cylinder and increases the ID (ignition delay) due to the reduced amount of oxygen (Jayabal et al., 2020). Venkatesan et al. (2021) investigated the properties of a 2-cylinder off-road vehicle CI engine

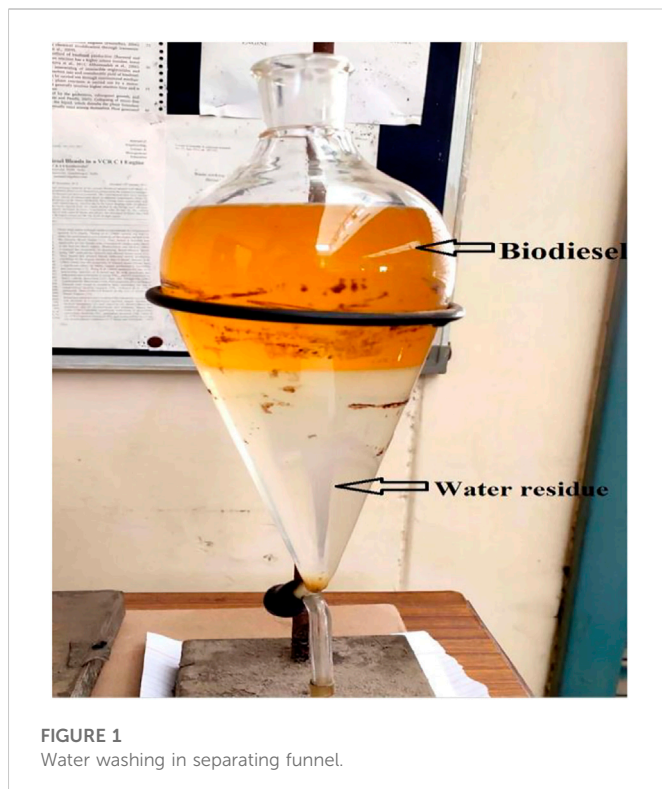


FIGURE 1
Water washing in separating funnel.

(Simpson S217-tractor) by using two types of fuel were used: P75SNB25 (Pine + soapnut biodiesel) and SNB20 (diesel + soapnut biodiesel) with a fixed rate of 10% EGR under varied loads. When comparing P75SNB25 blend fuel to diesel fuel without EGR, it was discovered that at full load, there is a reduction in surface (3.44%), EGT (3.90%), and HC (20%) emission for P75SNB25 blend fuel at 10% EGR. There is also an increase in BTE (4.44%) and CO (8%) emissions. When compared to diesel operation without EGR, the blend SNB20 with 10% EGR reduces EGT, HC, and NO_x emissions by 3.12%, 20%, and 10.55%, respectively. Shrivastava and Verma (2020) tested Roselle biodiesel combined with diesel in a CI engine, varying the FIP and load, and comparing the results to neat diesel. Boosting the FIP decreased the ID period, smoke emission, and thermal, and indicated efficiency while increasing the BSFC, EGT, cylinder pressure, and maximum rate of pressure increase, as well as CO₂ and NO_x emissions. At 220 bar FIP, CO₂ emissions increased by 1.6%, but NO_x and smoke emissions dropped by 3.18% and 2.20%, respectively, for RB20 blends compared to diesel fuel.

Previous research assessments found that biodiesel blend ratio, fuel injection pressure, and EGR all had a substantial influence on the diesel engine's characteristics. As is well known, these factors influence engine reactions in CI engines. These parameters must be considered to produce sensitive results in alternative fuel experiments. However, if any or all of the factors are taken into account, the number of tests required might be in the thousands. This is inefficient in terms of both cost and time. As a result, computer modelling applications have grown in popularity in recent years. The ability to model experiments with high accuracy while undertaking fewer experiments has proven valuable (Samet and Yeşilyurt, 2020). The goal of this study, among the multiple input factors, is to limit the number of experiments and construct a

mathematical model to produce optimal results. To decrease the number of trials, computer applications that can mimic many more experiments with a limited quantity of experimental data have been created. Among these programmes, RSM stands out owing to its capacity to optimise in less time since, unlike other apps, it develops the most appropriate matrix for testing. RSM is a statistical approach that produces and forms a model based on the correlation between output and certain under-control elements, capable of multivariate estimation and optimization (Srinidhi et al., 2021). Some research has been done on engine studies utilizing RSM-based models. Khanjani and Sobati (2021) utilized the RSM technique to investigate the influence of waste cooking oil biodiesel on the performance and combustion of a diesel engine. When compared to diesel fuel, engine torque decreased by 6.33%, but BP increased by 7.86%, and BSFC increased by 9.52%. CO, UHC, and NO_x emissions are also reduced by 42.86%, 34.02%, and 25.33%, respectively. Singh and Tirkey (2022) utilized RSM and ANOVA sensitivity testing to find the best engine operating conditions for dual-fueled engines driven by low-grade coal-based producer gas (PG) and diesel. According to RSM findings, the best values of the independent variables are equivalence ratio (0.12), CR (17.01), and engine load (12 kg). The measured optimal response values for BP (3.54 kW), BTE (28.23%), BSFC (0.38 kg/kWh), CO (0.38 kg/kWh), UHC (28.23%), CO₂ (0.0231% vol), and NO (4.2559 ppm). S Simsek et al. (2022) conducted an experiment to examine the effects of varying concentrations of graphene oxide (GO) on CI engine characteristics while using a 30% sesame oil (SO) + 70% diesel fuel combination with RSM to establish optimum operating parameters at various engine loads. Under optimal circumstances, the responses were 1,746.77 W, 968.73 g/kWh, 259.8°C, 0.0603%, 23.13 ppm, and 185.61 ppm for power, BSFC, EGT, CO, HC, and NO_x, respectively. According to the validation research, the maximum error between the optimal and experimental findings is 4.69%. According to the study's findings, it can be inferred that the RSM model can successfully represent a single-cylinder diesel engine, saving time and resources. RSM evaluated by Sharma et al. (2022) experimented with several fuels for the CI engine, including soya and soya ethanol mixes. According to RSM's studies, employing dual-fuel in a non-modified diesel engine improves engine performance and emissions. According to the conclusions of the investigation, an 8% soya biodiesel combination in dual fuel mode at 1486 RPM, 49.5 mm manometer airflow, and 6.27 kg engine load provides overall good engine performance. The emission parameters for BTE, VE, CO, HC, and NO_x are 24.29, 68.53%, 0.0715 vol. %, 51.6 ppmv, and 1,080 ppmv, respectively.

Following a study of the literature, it is concluded that there is a need for more research into the combined influence of blending ratio, FIP, EGR rate, and load on CRDI engine performance and emissions. Furthermore, the quantification of input parameters (% of SOME FIP, EGR rate, and load) for the desired outputs in terms of mathematical relations was not addressed for the selected combinations. Thus, the primary goal of this research article is to use modelling to optimise and explore the combined effect of different blending ratios, FIP, EGR rate, and load on engine performance and emissions, and to build an empirical link between output and input parameters. The novelty of this work is that it employs response surface methodology (RSM) to generate mathematical correlations between the independent variables and the responses, which were BSFC, BTE, CO, HC, and NO_x emissions levels. Thus, multifunctional research was carried out to decrease the greenhouse

TABLE 1 Physico-chemical Properties of different blends of Sesame biodiesel.

Properties	ASTM methods	Diesel (D100)	SesameMethyl ester (SOME)	D95SOME5	D90SOME10	D85SOME15	D80SOME20
Kinematics Viscosity (mm ² /sec) @40°C	D7042	2.9783	3.9256	3.0281	3.0742	3.1247	3.1694
Density (g/cm ³)	D7042	0.830	0.8810	0.8321	0.8348	0.8382	0.8413
Calorific value (MJ/kg)	D6751 37	42.1	39.65	41.96	41.82	41.69	41.62
Flashpoint (°C)	D0093	55	170	61	67	72	79
Fire point (°C)	D7094	64	192	70	77	83	90
Cloud point (°C)	D2500	-12	-6	-10	-9	-8	-7
Cetane number	D7668-17	51	54	51.2	51.3	51.5	51.6

gas effect and improve performance by utilising an ecologically friendly fuel, to acquire the best results with the least number of tests by optimising the working circumstances with RSM.

2 Materials and methodology

2.1 Biodiesel production

Sesame oil was purchased from a local vendor in New Delhi to extract sesame biodiesel. Biodiesel can be produced from raw sesame oil through the transesterification process. In the transesterification process, the triglycerides of the oil or fats are converted into ester on reaction with a small chain of alcohol in the presence of a catalyst, producing glycerol as a by-product. In this work, 200 mL of raw sesame oil was taken into a beaker. The temperature of raw sesame oil was increased to 120°C and maintained there for around 30 min while continually stirring to reduce the water contents in the oil. After that, the oil was put through a filter to separate solid particles and dirt. Potassium-methoxide was created by dissolving potassium hydroxide (KOH) in methanol at a 20:1 ratio. When the temperature of the oil was approximately 60°C, it was blended with a potassium-methoxide solution using a magnetic stirrer. The mixture was rapidly agitated and kept at 60°C for 90 min before being transferred to the settling container to begin the separation of glycerol from sesame biodiesel. Because glycerol is denser than biodiesel, it settles towards the bottom of the container. After the separation procedure had been completed for 24 h, the container's tap was opened, allowing the glycerol to drain (Bhatia et al., 2021).

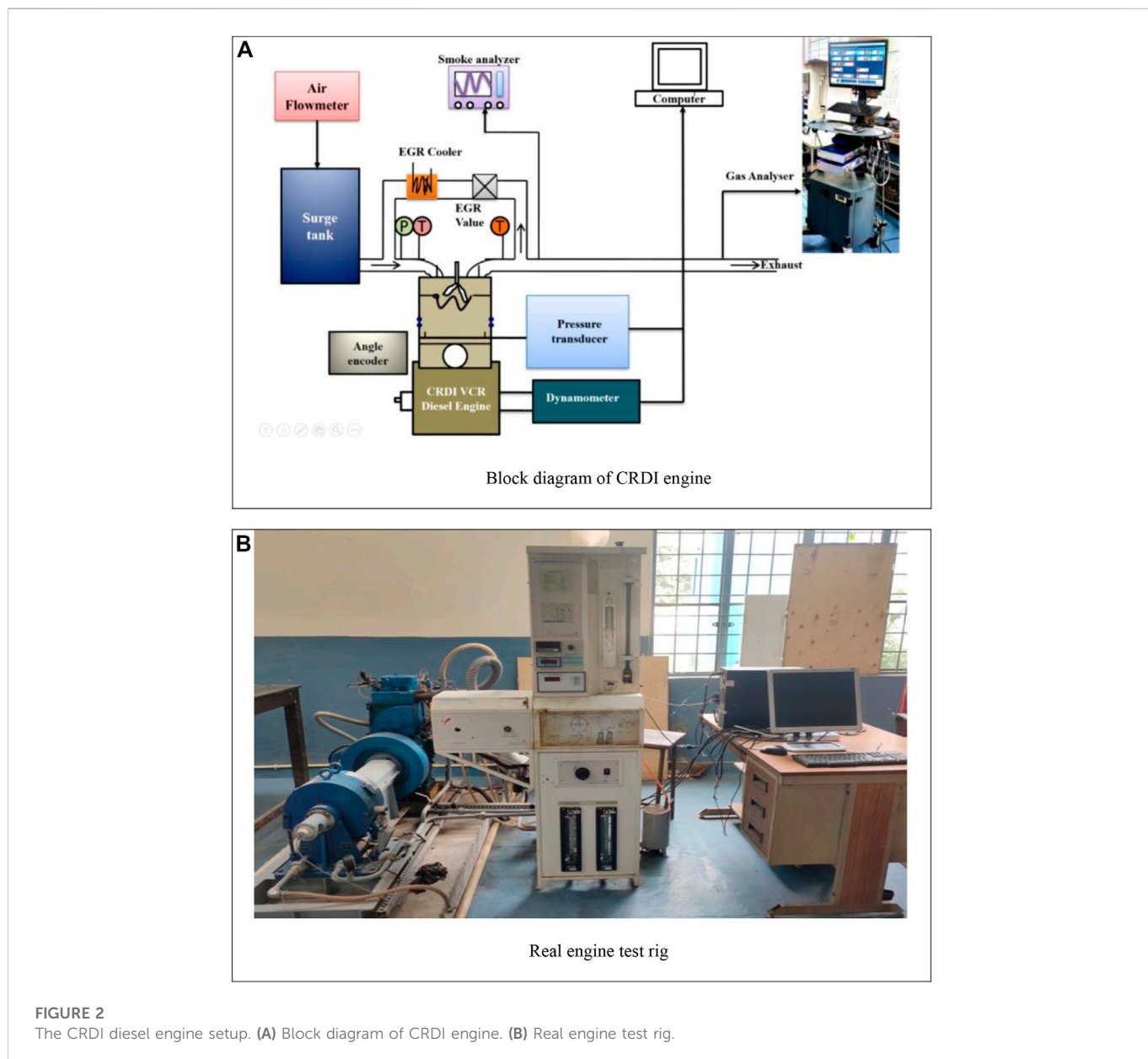
To eliminate residues of methanol and KOH from biodiesel, it was washed three times with warm water. The oil was placed in a settling container for 4 h after each wash to separate the washing residue from the biodiesel as shown in Figure 1. The amount of water utilized in each wash was about 10%–20% of the total amount of oil. After separation, the water evidence was removed by opening the tap. Finally, the produced biodiesel was heated to 110°C for around 30 min while stirring frequently to evaporate any remaining water content. It was observed that biodiesel yield was 88.4% achieved. The ASTM standard technique was used to determine the characteristics of fuels, which are described in Table 1. Details of the equipment's specifications used for fuel sample property measurement are shown in Table 2.

2.2 Experimental test rig

The experimental test setup is depicted in Figure 2. Experiments are conducted on CRDI diesel engine testing equipment at a constant speed of 1,500 rpm with a varying load to investigate the influence of fuel injection pressure, exhaust gas recirculation rate, and blend ratios on the emission and performance characteristics of the engine. The engine characteristics are shown in Table 3. To monitor RPM and load, the CRDI engine is utilised in conjunction with an Eddy current dynamometer. The cylinder pressure and temperature were measured using a pressure sensor and thermocouples, respectively. An exhaust gas analyzer was used to test exhaust gas emissions. Water was pumped through the engine block and cylinder head jackets to cool the engine. The "Engine Soft" lab view in a computer is used

TABLE 2 The Details of the equipment’s specifications used for fuel sample property measurement.

Property	Equipment	ASTM method	Precision
Kinematics viscosity and density	Stabinger Viscometer	ASTM D7042	±0.12 mm ₂ /s
Calorific value	Bomb calorimeter	ASTM 5865-13	±0.005 MJ/kg
Cetane number	Cetane number analyser	ASTM D613	±0.05
Flash point (°C) and Fire point	Pensky Martens Apparatus	ASTM D93	±0.2°C
Cloud point (°C)	Cloud point Tester	ASTM D2500/D97	±0.1°C



as an interface for all the equipment connected to it to capture output parameters. A low-pressure pump transports test fuel from the tank to a high-pressure CRDI pump, where it is filtered before entering the high-pressure pump. The injection time was set at 23 bTDC, and the

compression ratio to 18. An externally cooled EGR system was employed in this investigation. Cooled EGR minimises peak in-cylinder temperatures and hence avoids NO_x production by lowering the intake charge temperature.

TABLE 3 The technical specification of the CRDI diesel engine.

Model	Make Kirloskar CRDI VCR engine test
Engine	Single-cylinder, 4-stroke, Water cooled, Power 3.5 KW@ 1,500 rpm
Stroke length	110 mm
Bore diameter	87.5 mm
Compression ratio range	12–18
Dynamometer	Type eddy current, water-cooled with loading unit
Common rail	With pressure sensor and pressure regulating valve
EGR	Water cooled, SS, Range 0%–15%
Fuel tank	Capacity 15 lit, with fuel metering pipe of glass
Software	“Enginesoft” Engine performance analysis software
Airflow transmitter	Make Wika Germany, Pressure transmitter, Range (–) 250 mm WC
Load sensor	Make VPG Sensotronics, Load cell, type strain gauge, range 0–50 Kg
Overall dimensions	W 2000 mm × D 2500 mm × H 1500 mm

TABLE 4 Accuracy of different measurement instruments.

Measuring parameter	Accuracy	% Uncertainty
Brake thermal efficiency (BTE)	—	±0.5
Brake-specific fuel consumption (BSFC)	—	±0.4
Speed indication	±0.05%	±0.2
Exhaust gas temperature	±2%	±1
Dynamometer	±2%	±0.1
Pressure sensor	±1	±0.3
CO emission	±0.01 vol%	±0.3
HC emission	±5 ppm	±0.6
NOx emission	±10 ppm	±0.8

TABLE 5 The input variables with their levels.

Parameters	Levels				
	–2	–1	0	+1	+2
SOME ratio (%)	0	5	10	15	20
Fuel injection pressure (bar)	500	525	550	575	600
EGR (%)	0	3.5	7	10.5	14
Load (kg)	0	3	6	9	12

2.3 Uncertainty analysis

Estimating the percentage of mistakes can be used to estimate the accuracy of experimental results. Experiments are prone to errors owing to instrument calibration, environment, and observations. The experimental data's error evaluations are computed using systematic

equations. To estimate the real value, the uncertainty analysis uses the average of repeat measurements. For the error analysis, the mean of six observations of a given parameter was used. All of the engine parameters include error bars to show the degree of uncertainty in the stated measurement. Table 4 compares the accuracy of several measuring devices.

A popular mathematical equation is used to determine many unidentified uncertainties from well-established quantities (Chaitanya and Mohanty, 2022). The square root technique is used to assess the correctness of these results as shown in Eq. 1.

$$\frac{U_y}{y} = \sqrt{\sum_{i=1}^n \left(\frac{1}{y} \frac{\partial y}{\partial x_i} \right)^2} \quad (1)$$

In the following formula, the symbol “U_y” denotes the deviation or uncertainty in the word “y,” which is reliant on the other component (x_i). Five observations are reported in this experimental study under varied engine running settings. Repeated experiments are used to calculate the uncertainty for variables such as BTE, BSFC, HC, CO, and NOx. The following table summarises the experiment's uncertainty when all variables' errors are taken into account:

The uncertainty of the test

$$\begin{aligned} &= \pm \sqrt{(\text{BTE})^2 + (\text{BSFC})^2 + (\text{CO})^2 + (\text{HC})^2 + (\text{NOx})^2} \\ &= \pm \sqrt{(0.5)^2 + (0.4)^2 + (0.3)^2 + (0.6)^2 + (0.8)^2} \\ &= \pm 1.22\% \end{aligned}$$

The uncertainty levels of each component of equipment were calculated. The total uncertainty of the present experiment was determined to be 1.22%, which is significantly lower than the 5%. It is generally understood that the allowable range for uncertainty is less than the stated amount. As a result, the total uncertainty of the system was within reasonable parameters.

TABLE 6 The actual values of independent variables along with their output responses.

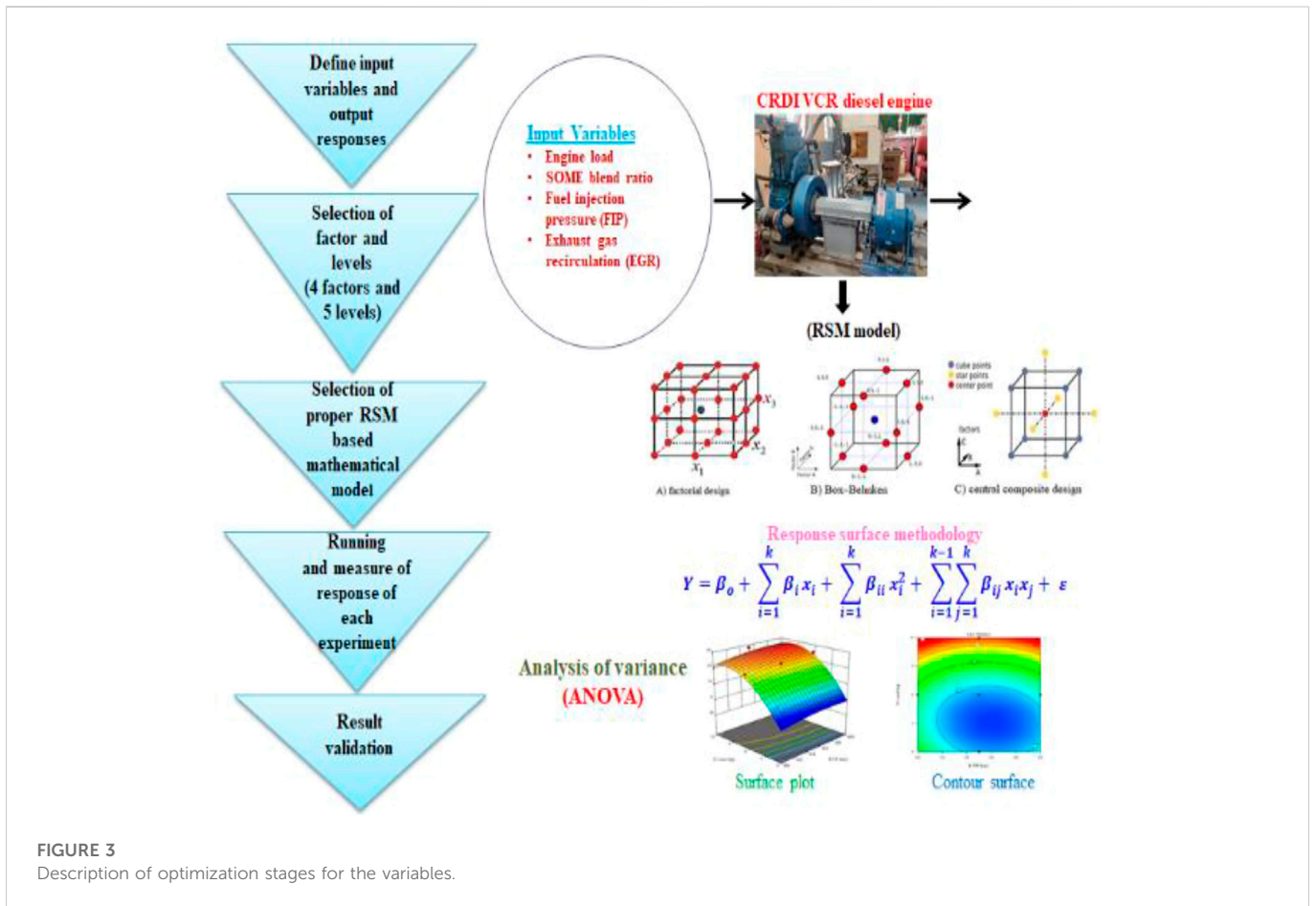
S. No.	Blend (%)	FIP (bar)	EGR (%)	Load (kg)	BTH (%)	BSFC (kg/kWh)	CO % vol.	HC ppm	NOx ppm
1	15	575	10.5	9	24.1596	0.3406	0.343	28	629
2	10	550	7.0	6	23.1228	0.3816	0.1568	22	419
3	10	550	7.0	6	23.1228	0.3816	0.1568	22	419
4	10	550	14.0	6	22.0428	0.3963	0.2058	28	326
5	15	525	10.5	3	9.7848	0.4331	0.392	19	247
6	5	525	10.5	3	10.1844	0.4221	0.3038	24	216
7	15	575	10.5	3	12.1608	0.4331	0.098	15	266
8	5	525	3.5	9	25.4124	0.3196	0.5096	34	680
9	5	525	10.5	3	10.1844	0.4221	0.3038	24	216
10	10	550	7.0	0	0.432	0.66	0.049	13	175
11	10	550	7.0	6	23.1228	0.3816	0.1568	22	419
12	10	550	0.0	6	23.6628	0.367	0.1176	19	485
13	5	575	3.5	9	27.7884	0.3196	0.4606	30	691
14	10	550	7.0	6	23.1228	0.3816	0.1568	22	419
15	10	550	7.0	12	28.188	0.3045	0.7448	40	837
16	15	575	3.5	3	13.1544	0.4167	0.0588	13	359
17	5	575	10.5	9	26.6112	0.3322	0.5194	24	598
18	0	550	7.0	6	26.892	0.36	0.3038	23	394
19	5	575	10.5	3	12.5604	0.4221	0.2744	20	235
20	10	500	7.0	6	22.1508	0.3816	0.294	27	408
21	10	600	7.0	6	25.1748	0.389	0.2156	19	444
22	5	525	10.5	9	24.2352	0.3322	0.5488	37	480
23	10	550	7.0	6	23.1228	0.3816	0.1568	22	419
24	10	550	7.0	6	23.1228	0.3816	0.1568	22	419
25	15	525	3.5	9	22.7448	0.3278	0.3332	29	704
26	15	575	3.5	9	25.0884	0.3278	0.3038	25	722
27	15	525	10.5	9	21.7836	0.3406	0.3724	29	611
28	5	575	3.5	3	13.6512	0.4062	0.2352	17	328
29	10	550	7.0	6	23.1228	0.3816	0.1568	22	419
30	15	525	3.5	3	10.7784	0.4167	0.0882	16	340
31	20	550	7.0	6	21.438	0.3887	0.0588	15	456

3 Response surface methodology

3.1 RSM model and experimentation

A response surface approach is a strong tool for optimizing process parameters in different research areas such as manufacturing, I C engine, microbial product, the medical sector, and so on. This method combines statistical and mathematical techniques for model creation, analyzing the influence of several independent variables, and determining optimal variable values. The RSM model was developed using data from the experimental investigation. The primary goal is to investigate the relationship between the responses and the input factors

to reduce or optimise the response attributes. It can both develop and show a simple equation for the parameters to be optimised using a small amount of experimental data. Furthermore, it is an application that may use analysis of variance to determine the influence of working parameters on outputs (ANOVA) (S Uslu et al., 2022, S Sathyanarayanan et al., 2022). The RSM with DoE has been demonstrated to be an effective modelling technique. As a result, in the current study, RSM with “Minitab 20” was proposed for establishing the connection between the identified variables and the responses (Chelladurai et al., 2021). This technique not only saves money and time but also provides the necessary knowledge on interaction effects with a lesser number of tests.



For each of the four input variables, five levels were chosen in this experiment. The discovered variables and their levels are shown in Table 5. Table 6 summarises the data obtained for performance metrics such as BTE and BSFC, as well as emission characteristics such as HC, CO, and NOx, during the current study.

The RSM technique of optimization entails three key steps: statistically constructing the experiments, predicting the coefficients in a mathematical model, forecasting the response, and verifying the model’s appropriateness (Eq. 2) inside the experimental setup (Figure 3).

$$S = f(X_1, X_2, X_3, \dots, X_n) \tag{2}$$

where S denotes the system response and X_n denotes the component of action. One useful aspect of RSM is the ability to use the analysis of variance (ANOVA) approach to create an appropriate model between the response and independent variables. The 2nd order mathematical model presented in Eq. 3 may be used to calculate S and it is stated as follows (Pereira et al., 2021, MK Yesilyurt et al., 2022):

$$S = a_0 + \sum_{i=1}^k a_i x_i + \sum_{i=1}^k a_{ii} x_i^2 + \sum_{i=1}^{k-1} \sum_{j=1}^k a_{ij} x_i x_j + \epsilon \tag{3}$$

where S is the response, a_0 is the average of the responses, and a_i , a_{ii} , and a_{ij} are the response coefficients. The 2nd, 3rd, and 4th terms, respectively, indicate linear, higher-order, and interaction effects and ϵ is the error.

In this research, the influence of four factors on the efficiency and exhaust of a CRDI engine is evaluated in order of importance: SOME %, FIP, EGR, and engine load. A central composite design (CCD) with the face in the centre is chosen. Because it allows for the construction of a 2nd order model for the response, the CCD is most commonly used to obtain the response surface. This sort of design occurs when the distances from both axial points, which serve as the CCD’s factorial points, to the centre are the same central distance, resulting in the same chances in the available response at all places of a centred sphere at the origin. The following correlation (Eq. 4) is used to calculate the number of points necessary for the four parameters under consideration (Rejeb et al., 2021):

$$N = 2^k + 2k + a_0 = 2^4 + 2*4 + 7 = 31 \text{ trials} \tag{4}$$

where N signifies the number of runs, k is the number of variables, and a_0 is the number of repetitions at the central design point.

3.2 ANOVA results

When determining the relevance of a mathematical model, the most commonly used statistical procedures are analysis of variance (ANOVA) as shown in Tables 7, 8. When there are more than two treatments, ANOVA is used. The p -value is defined as the choice of elimination points for the null

TABLE 7 ANOVA of the developed models for BTE and BSFC.

Sources	DF	BTE (%)		BSFC (kg/kWh)	
		F-value	p-value	F-value	p-value
Model	14	27.45	0.000	7.96	0.000
Linear	4	80.40	0.000	23.63	0.000
BLEND (%)	1	5.67	0.030	0.62	0.443
FIP (bar)	1	8.08	0.012	0.00	0.994
EGR (%)	1	1.32	0.267	1.11	0.307
Load (Kg)	1	306.54	0.000	92.80	0.000
Square	4	15.24	0.000	4.22	0.016
BLEND (%)*BLEND (%)	1	0.54	0.474	1.43	0.250
FIP (bar)*FIP (bar)	1	1.19	0.292	0.51	0.484
EGR (%)*EGR (%)	1	2.78	0.115	0.77	0.394
Load (Kg)*Load (Kg)	1	60.17	0.000	12.42	0.003
2-Way Interaction	6	0.29	0.935	0.01	1.000
BLEND (%)*FIP (bar)	1	0.02	0.883	0.02	0.898
BLEND (%)*EGR (%)	1	0.00	0.955	0.02	0.889
BLEND (%)*Load (Kg)	1	1.63	0.220	0.00	0.961
FIP (bar)*EGR (%)	1	0.02	0.890	0.02	0.898
FIP (bar)*Load (Kg)	1	0.02	0.883	0.02	0.898
EGR (%)*Load (Kg)	1	0.02	0.878	0.00	0.987
Modal					
SD (Standard deviation)		1.87562		0.0305708	
R ²		96.00%		87.45%	
Adjusted R ²		92.51%		76.47%	
Predicted R ²		76.98%		27.70%	

hypothesis to be rejected at the lowest degree of significance. For analysis, the level of significance must be specified; for example, 5% ($p < 0.05$) to show that the treatments vary statistically. From Table 6, it was found that the p -value of blend%, FIP, and load is less than 0.05 for BTE and only load for BSFC. It means that blend %, FIP, and load have a great impact on the response BTE and for BSFC, engine load plays a significant role. Similarly in Table 7, it was observed from the p -value that blend%, EGR, and load have a great effect on CO emission. The blend %, FIP, and load have more impact on HC emission. The load and EGR have more impact on NOx emission. As a consequence, when “ p ” determined by ANOVA is less than the level of significance, the results can be regarded significant; but, when “ p ” is larger than the level of significance, the null hypothesis is true and the results are not substantially different, so there are no reasons to reject it (Kumar et al., 2021a).

Tables 7, 8 also show the coefficient of determination (R^2) for created models, demonstrating an excellent connection between the experimental and projected values of the feature. The

correlation between experimental and predicted values for BTE ($R^2 = 0.96$), BSFC ($R^2 = 0.8745$), CO ($R^2 = 0.8973$), HC ($R^2 = 0.9524$), and NOx ($R^2 = 0.9856$) was found to be excellent. The adjusted R^2 is a variant of R^2 that has been updated to account for the number of predictors in the model. BTE (adj. $R^2 = 0.9251$), BSFC (adj. $R^2 = 0.7647$), CO (adj. $R^2 = 0.8075$), HC (adj. $R^2 = 0.9107$), and NOx (adj. $R^2 = 0.9730$) have high adjusted R^2 values, indicating that these models are very accurate (Mutuk and Mesci, 2014; Pamnani et al., 2017).

3.3 Optimization and desirability approach

The optimization of real-world issues necessitates the use of numerous answers of interest. Techniques utilized include overlaying the contour plots for each answer, restricted optimization problems, and the desirability technique. The desirability technique is shown to offer advantages such as simplicity, software availability, and flexibility in weighing and

TABLE 8 ANOVA of the developed models for CO, HC, and NOx emission.

Sources	DF	CO (%)		HC (ppm)		NOx (ppm)	
		F-value	p-value	F-value	p-value	F-value	p-value
Model	14	9.99	0.000	22.86	0.000	78.10	0.000
Linear	4	25.66	0.000	73.30	0.000	266.01	0.000
BLEND (%)	1	21.72	0.000	29.71	0.000	16.95	0.001
FIP (bar)	1	4.05	0.061	34.46	0.000	8.97	0.009
EGR (%)	1	4.28	0.055	7.43	0.015	63.03	0.000
Load (Kg)	1	72.60	0.000	221.58	0.000	975.10	0.000
Square	4	8.32	0.001	4.75	0.010	5.82	0.004
BLEND (%)*BLEND (%)	1	1.81	0.197	2.57	0.129	0.70	0.415
FIP (bar)*FIP (bar)	1	7.30	0.016	1.31	0.269	0.78	0.389
EGR (%)*EGR (%)	1	0.97	0.339	2.21	0.156	0.01	0.918
Load (Kg)*Load (Kg)	1	28.30	0.000	12.58	0.003	22.58	0.000
2-Way Interaction	6	0.66	0.686	1.32	0.305	1.02	0.447
BLEND (%)*FIP (bar)	1	0.50	0.488	4.22	0.057	2.83	0.112
BLEND (%)*EGR (%)	1	0.96	0.342	1.05	0.320	0.02	0.901
BLEND (%)*Load (Kg)	1	0.50	0.488	1.05	0.320	0.00	1.000
FIP (bar)*EGR (%)	1	0.50	0.488	0.26	0.615	0.02	0.901
FIP (bar)*Load (Kg)	1	0.96	0.342	0.26	0.615	0.00	0.972
EGR (%)*Load (Kg)	1	0.50	0.488	1.05	0.320	3.27	0.090
Modal							
SD (Standard deviation)		0.0725444		1.94722		27.6641	
R ²		89.73%		95.24%		98.56%	
Adjusted R ²		80.75%		91.07%		97.30%	
Predicted R ²		40.87%		72.58%		91.69%	

assigning priority to individual responses. In this study, a desirability approach based on the response surface technique is utilized to optimize experiment parameters (SOME%, FIP, EGR, and load) for the measured characteristics of responses (maximize BTE, and minimize BSFC, CO, HC, and NOx). The optimization research is finished. The optimization research was carried out using MINITAB 20, in which each response is converted to a dimensionless desirability value (d) ranging between $d = 0$, indicating that the response is completely undesirable, and $d = 1$, indicating that the response is more desirable (Sharma et al., 2022). It was discovered that the desirability approach for this investigation achieved 0.7954.

Figure 4 depicts the outcomes of the RSM optimization method. When the test engine fuel input variables were set to 20% sesame biodiesel blend ratio, FIP 577.5 bar, EGR 5.26%, and load 5.13 kg, the best value of output variables was BTE (18.92%), BSFC (0.3705 kg/kWh), CO (0.03% vol.), HC (13 ppm), and NOx (447.5 ppm).

4 Result and discussion

In the current investigation, the impacts of experiment factors such as SOME%, FIP, EGR, and load on BTE, BSFC, CO, HC, and NOx were investigated. Table 5 displays the experimental responses of 31 runs in the design matrix, as well as the points on RSM-fitted models that correspond to them. 3-D surface view plots and accompanying contour plots were created using the four independent components. Two items were considered at a time in these plots, with the other two factors staying in the middle level and serving as hold parameters.

4.1 Interactive effect of various input factors on brake thermal efficiency (BTE)

BTE refers to the combustion system's ability to take the test fuel and gives a comparable method for determining how efficiently the fuel's energy was transferred to mechanical work. Eq. 5 are provided in

the independent factors' 2nd-order equations to recognise the BTE created by MINITAB 20.

$$\begin{aligned}
 BTE (\%) = & 223 + 0.58 BLEND (\%) + 0.733 FIP (bar) \\
 & + 1.02 EGR (\%) + 6.82 Load (Kg) \\
 & - 0.0103 BLEND (\%) * BLEND (\%) \\
 & - 0.000612 FIP (bar) * FIP (bar) \\
 & - 0.0478 EGR (\%) * EGR (\%) \\
 & - 0.3023 Load (Kg) * Load (Kg) \\
 & - 0.00056 BLEND (\%) * FIP (bar) \\
 & - 0.0015 BLEND (\%) * EGR (\%) \\
 & - 0.0399 BLEND (\%) * Load (Kg) \\
 & - 0.00076 FIP (bar) * EGR (\%) \\
 & - 0.00094 FIP (bar) * Load (kg) \\
 & - 0.0069 EGR (\%) * Load (Kg)
 \end{aligned} \tag{5}$$

Figure 5 shows the cumulative impact of various input variables on the BTE. Figure 5 (i) a and (i) b represent the surface plot and contour surface for the change in BTE due to variation in biodiesel ratio (sesame oil methyl ester) and EGR. The BTE of the engine was shown to decrease as the percentage of biodiesel in the blends increased. This might be due to biodiesel's higher oxygen content, which may have resulted in improved combustion as compared to pure diesel. Furthermore, all biodiesel blends exhibited lower BTE, which might be attributed to biodiesel's much worse efficiency, particularly at lower CR, due to a loss in calorific value and increased fuel consumption. When the EGR was increased during the SOME/diesel mix-driven CRDI operation, the BTE fell somewhat, which is almost definitely owing to the charge dilution influence decreasing combustion quality. Kumar et al. (2021b) found a similar trend when testing linseed biodiesel blends in CRDI engines.

Figure 5 (ii) a and (ii) b illustrate the surface plot and contour surface for the effect of blend% and FIP on the BTE. The BTE improves as injection pressure rises at full load, as seen in the graph. By raising the fuel injection pressure, the degree of atomization is enhanced. This is because finer atomization reduces ignition delay by increasing the surface volume ratio. The 3-D response curves for the impact of SOME% and engine load are shown in Figure 5 (iii) a and (iii) b. Due to an increase in brake power, the BTE for diesel and biodiesel blends increases as the load increases. The highest efficiency for D90SOME10 test fuel operating at 550 bar FIP and 7% EGR rates were observed to be at a 12 kg load. Figure 5 (iv) a and (iv) b show the response surface graph for the effect of load and FIP on BTE.

4.2 Interactive effect of various input factors on brake-specific fuel consumption (BSFC)

The quantity of fuel required by the engine to create a unit power output is specified as BSFC. It is a measure of the combustion efficiency of the fuel. Eq. 6 are shown in the 2nd order equations obtained in the independent factors to recognise the BSFC created by MINITAB 20.

$$\begin{aligned}
 BSFC \left(\frac{kg}{kWh} \right) = & -1.33 + 0.0015 BLEND (\%) + 0.0070 FIP (bar) \\
 & + 0.0007 EGR (\%) + 0.0545 Load (Kg) \\
 & - 0.000273 BLEND (\%) * BLEND (\%) \\
 & - 0.000007 FIP (bar) * FIP (bar) \\
 & - 0.000409 EGR (\%) * EGR (\%) \\
 & - 0.002238 Load (Kg) * Load (Kg) \\
 & - 0.000008 BLEND (\%) * FIP (bar) \\
 & - 0.000062 BLEND (\%) * EGR (\%) \\
 & - 0.000025 BLEND (\%) * Load (Kg) \\
 & - 0.000011 FIP (bar) * EGR (\%) \\
 & - 0.000013 FIP (bar) * Load (kg) \\
 & - 0.000012 EGR (\%) * Load (Kg)
 \end{aligned} \tag{6}$$

Figure 6 depicts the 3D response curves displayed with the interaction impacts of the process variable on the BSFC utilizing the design of expert (DOE) software against any two independent variables while maintaining other variables at their zero level. Figure 6 (i) a and (i) b demonstrate the impact of sesame biodiesel% and EGR rates on BSFC through response surface curves. It was discovered that when the proportion of SOME biodiesel in the test fuel increases, the BSFC value first gets increases. The main reason for this is that the calorific value of biodiesel declines as the proportion of biodiesel in blends increases, necessitating an increase in

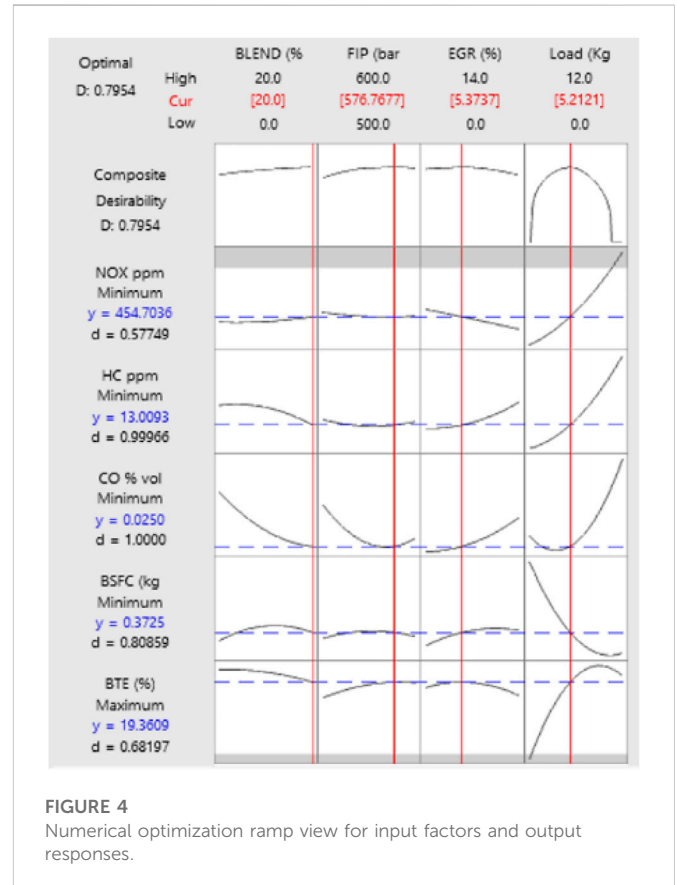


FIGURE 4 Numerical optimization ramp view for input factors and output responses.

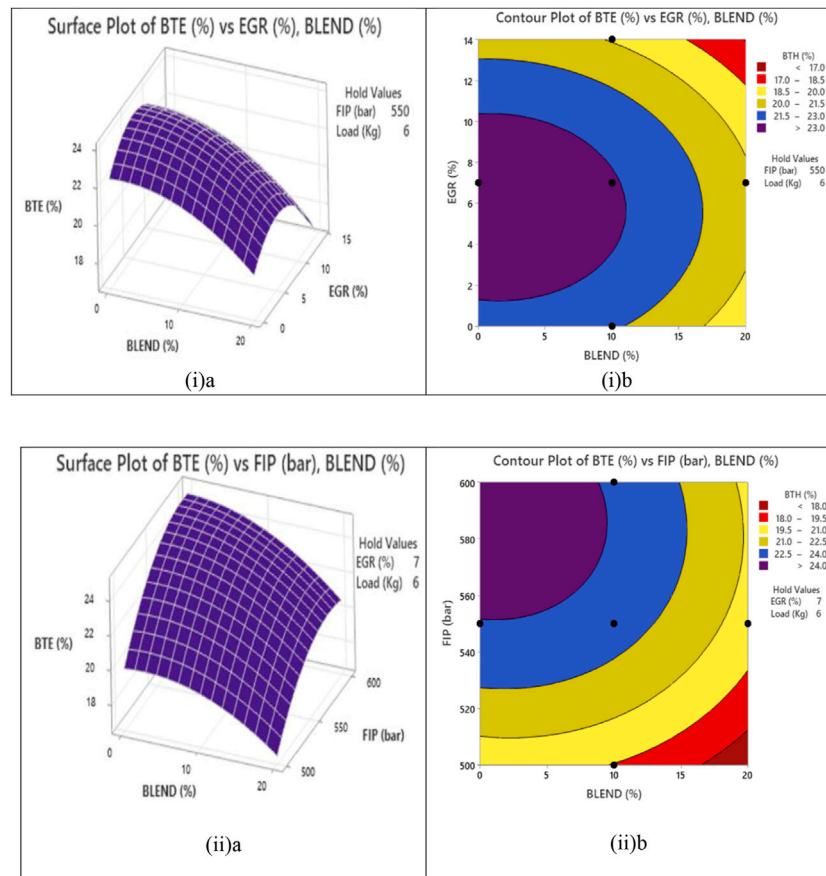


FIGURE 5
Effect of input factors on BTE.

blend flow rate to maintain the same operating conditions in terms of power output for all test fuels. After 10% SOME, BSFC values gets decreased as shown in graph. Because oxygen enhances combustion efficiency, it takes up space in the mix and so slightly raises the apparent fuel consumption rate noticed when running a biodiesel engine. These findings are consistent with comparable observations recorded by Sharif et al. (2020) after testing *Nodularia Spumigena* microalgae in a diesel engine versus different vegetable oil derived biodiesel. The combined effect of blend ratio and EGR on BSFC are described in Figure 6 (i) a and (i) b through response surface and contour plot. The value of the BSFC rises as the EGR levels increase. This is because when the EGR rate increases, the combustion temperature, and oxygen concentration fall, leading combustion to degrade. Additionally, when the EGR rate increases, so do the combustion time, but volumetric combustion decreases, resulting in increased fuel consumption.

The combined effect of blend ratio and FIP on BSFC is depicted in Figure 6 (ii) a and (ii) b through response surface and contour plot. With an increase in FIP, the BSFC values decreased. This might be due to finer atomization and better mixing at greater FIP. Figure 6 (iii) a and (iii) b depict the change in BSFC at various blend% and engine loads. According to the result obtained, raising the engine load from zero to full load results in a declining trend in the BSFC. This might be owing to better atomization at greater pressures, which allows for a rapid rate of heat release. The impact of load and FIP on the variation of BSFC illustrates in Figure 6 (iv) a and (iv) b.

4.3 Interactive effect of various input factors on carbon dioxide (CO) emission

Carbon monoxide is produced when there is insufficient oxygen for the combustion cycle yet the fuel-air mixture is high enough for combustion to proceed in the engine. Because there is not sufficient oxygen for carbon to be converted to CO_2 , some of the fuel is not burned and some carbon is turned into CO. Poor mixing, concentrated rich patches, inefficient burning, and an inadequate supply of oxygen all contribute to carbon monoxide emissions. Eq. 7 are shown in the independent factors' 2nd-order equations to recognise the reactions to CO emission created by MINITAB 20.

$$\begin{aligned}
 CO(\% \text{ vol.}) = & +15.67168 + 0.085514 \text{ blend}(\%) - 0.058899 \text{ FIP}(\text{bar}) \\
 & + 0.171122 \text{ EGR}(\%) - 0.068449 \text{ load}(\text{kg}) \\
 & - 0.000188 \text{ blend} * \text{ FIP} + 0.000283 \text{ blend} * \text{ EGR} \\
 & - 0.001570 \text{ blend} * \text{ load} - 0.000293 \text{ FIP} * \text{ EGR} \\
 & + 0.000094 \text{ FIP} * \text{ load} - 0.002445 \text{ EGR} * \text{ load} \\
 & + 0.000660 \text{ blend} * \text{ blend} + 0.000056 \text{ FIP} * \text{ FIP} \\
 & + 0.000946 \text{ EGR} * \text{ EGR} + 0.007821 \text{ load} * \text{ load}
 \end{aligned}
 \tag{7}$$

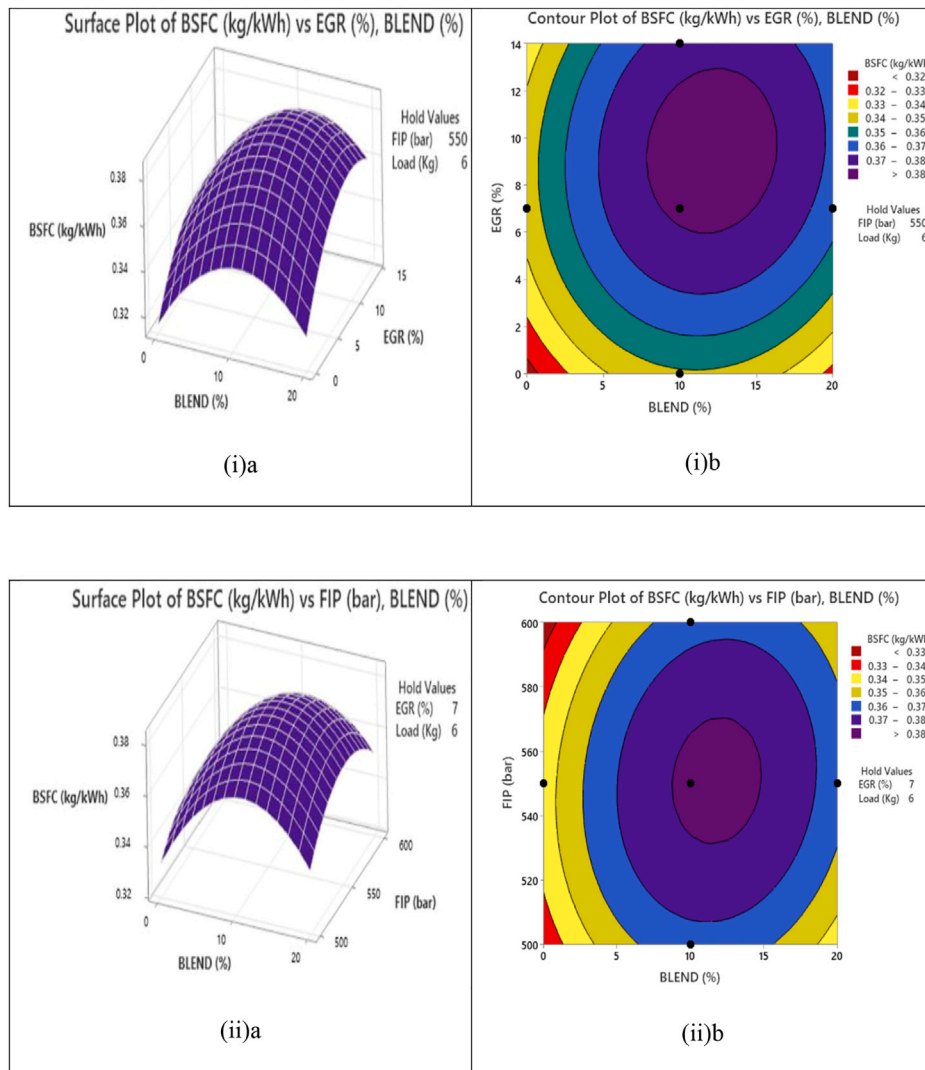


FIGURE 6
Effect of input factors on BSFC.

The interaction impact of all control settings on carbon monoxide emissions is depicted in Figure 7. Figure 7 (i) a and (i) b show the combined effect of mix ratio and EGR. Because of their increased oxygen content, biodiesel blends were shown to have reduced CO emissions when utilized as a test fuel. The presence of more oxygen in the fuel promotes complete combustion, resulting in decreased CO emissions. It was also demonstrated that raising EGR rates on a CRDI engine decreases CO oxidation owing to decreased oxygen concentrations, resulting in a modest increase in CO emissions.

Figure 7 (ii) a and (ii) b depicts the variation in CO emission at various blend% and FIP. Based on this graph, it was determined that increasing injection pressure reduced CO emissions in the CRDI diesel engine. The greater the FIP, the better the fuel-air mixing and the easier and more thorough combustion of the tiny droplets. CO emissions are reduced as a result of these effects. These findings are congruous with Kim et al. (2019), who got a similar outcome by using a diesel/biodiesel blend with FIP.

Figure 7 (iii) a and (iii) b show the combined effect of blend percentage and load on CO emission *via* a response surface and contour plot. CO emissions are higher at low engine load than at high engine load, as can be observed. The higher the engine load, the lower the CO emissions for all fuels. This is due to increased evaporation and mixing of air and fuels, resulting in greater in-cylinder temperatures. Figure 7 (iv) a and (iv) b show the influence of FIP and load on CO emission variation using 3-D response curves.

4.4 Interactive effect of various input factors on hydrocarbon (HC) emission

Increased HC emissions occur from improper combustion of fuel particles. Eq. 8 are shown in the independent factors' 2nd-order equations in order to recognise the responses HC provided by MINITAB 20.

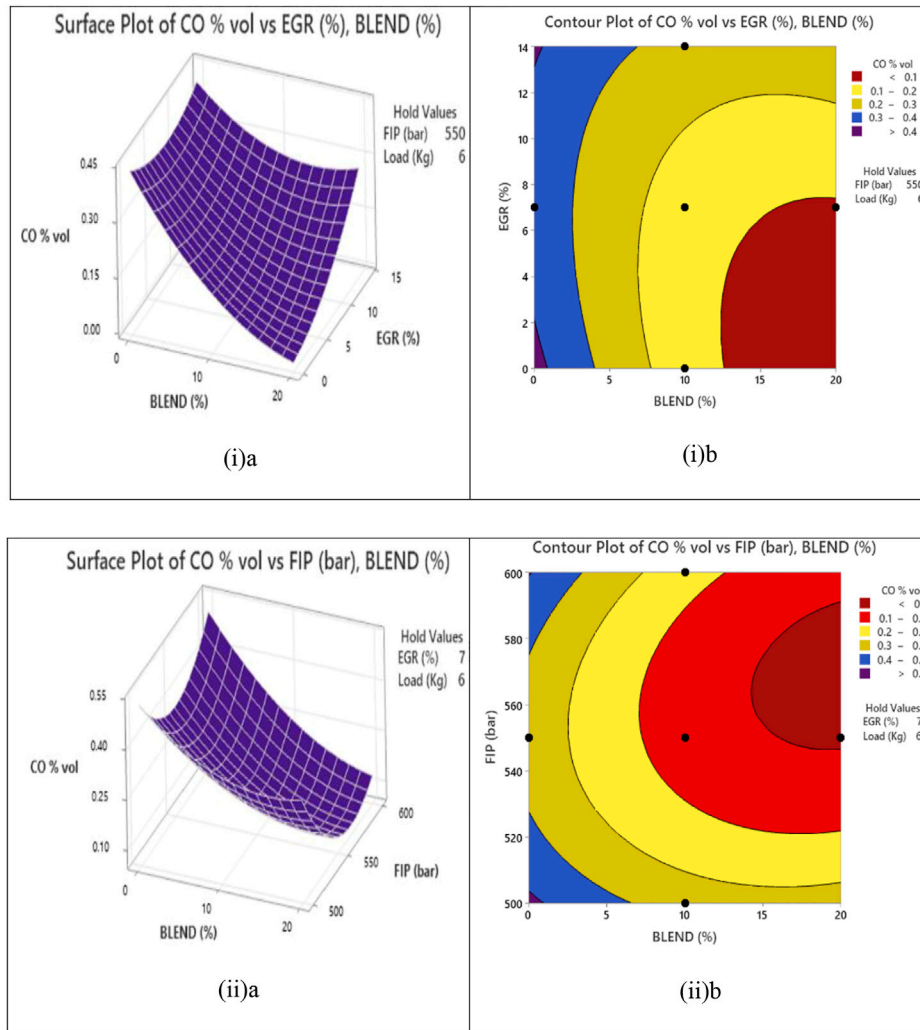


FIGURE 7
Effect of input factors on carbon dioxide (CO) emission.

$$\begin{aligned}
 HC (ppm) = & +224.54756 - 3.19443 \text{ blend} (\%) - 0.706461 \text{ FIP} (\text{bar}) \\
 & + 3.35396 \text{ EGR} (\%) + 4.70373 \text{ load} (\text{kg}) \\
 & + 0.005686 \text{ blend} * \text{FIP} + 0.013294 \text{ blend} * \text{EGR} \\
 & + 0.014053 \text{ blend} * \text{load} - 0.005913 \text{ FIP} * \text{EGR} \\
 & - 0.007189 \text{ FIP} * \text{load} - 0.073081 \text{ EGR} * \text{load} \\
 & - 0.025261 \text{ blend} * \text{blend} + 0.000590 \text{ FIP} * \text{FIP} \\
 & + 0.040283 \text{ EGR} * \text{EGR} + 0.138163 \text{ load} * \text{load}
 \end{aligned}
 \tag{8}$$

Figure 8 shows the 3D response curves with the interaction impacts of the process variable on the HC emission using the design of the expert (DOE) programme against any two independent variables while keeping the other variables at their zero levels. Figure 8 (i) a and (i) b demonstrate the fluctuation in HC emission owing to blend% and EGR using the contour surface and surface plot. The quantity of HC emissions decreases as the fraction of SOME biodiesel blends increases at all engine loads due to the increased oxygen content and higher CN. Because of the efficient atomization of the fuel, the decreased HC emission ensures that the

combustion is great. In CRDI diesel engines, raising the EGR percentage increased HC emissions. This tendency might be attributed to the charge’s diluting influence on EGR use, which causes incomplete combustion and lowers BTE. Increased EGR rates can cause lower flame temperatures, leading to bigger flame-quenching zones where combustion is difficult. Appavu et al. (2021) found a similar trend when studying the effect of EGR on the emission of diesel engines.

Figure 8 (ii) a and (ii) b show the change in HC emission as a function of blend percentage and FIP value. As demonstrated in the graph, increasing injection pressure lowered HC emissions. When the injection pressure was increased, the fuel-air mixing in the combustion chamber improved, resulting in reduced UHC emissions than when the injection pressure was low. Figure 8 (iii) a and (iii) b show the surface plot and contour surface of HC emission as a function of blend ratio and load. When it comes to engine load, HC grows as the load rises since there is a greater replacement of biodiesel, resulting in maximum combustion of the biodiesel/diesel mix fuel. High HC levels were also caused by flame quenching and incomplete combustion. Figure 8 (iv) a and (iv) b

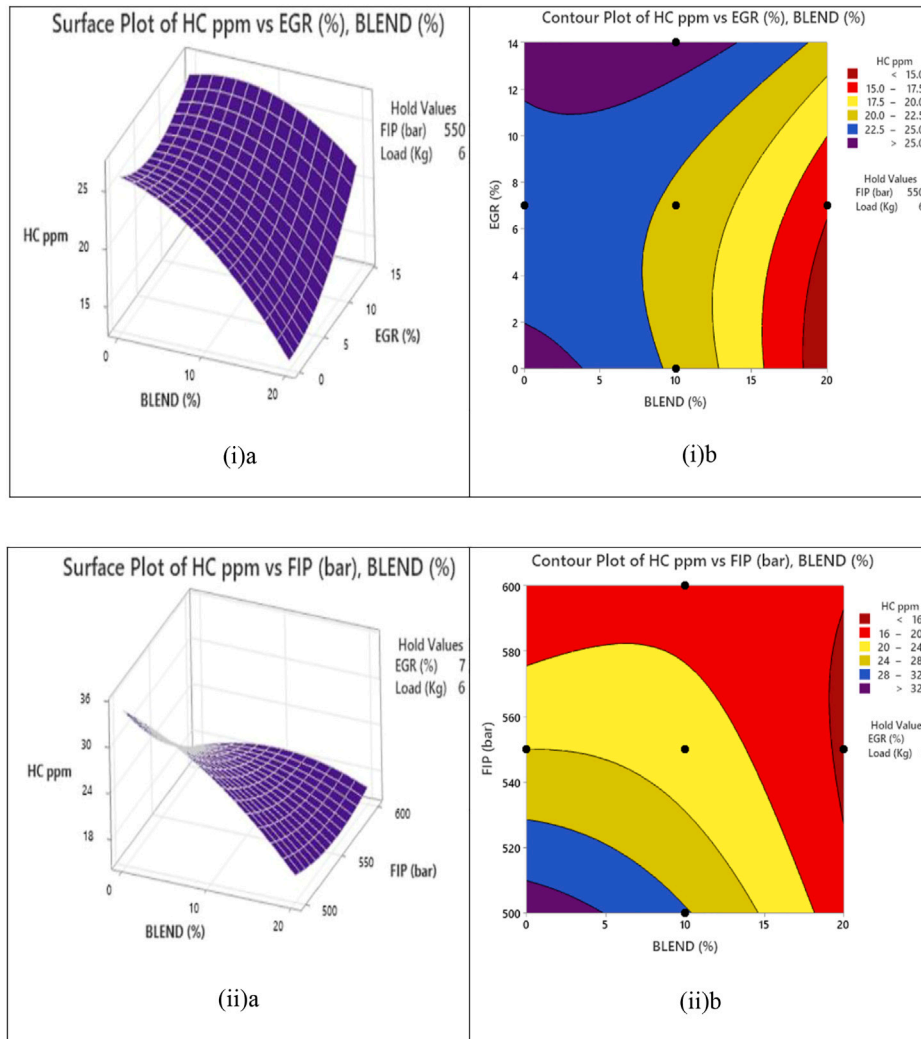


FIGURE 8
Effect of input factors on HC emissions.

show the effect of FIP and load on the variation of HC emission through response surface graphs.

4.5 Interactive effect of various input factors on the oxide of nitrogen (NOx) emission

This is the most significant property of biodiesel and its blend in terms of emissions. Because NOx is the most hazardous gaseous emission from engines, engine researchers are always working to reduce it. The term “thermal NOx” refers to NOx produced in a combustion chamber by the high-temperature oxidation of nitrogen (N₂). The production of NOx is strongly dependent on the temperature, oxygen content, and reaction time in the cylinder. Eq. 9 are depicted in the 2nd order equations acquired in the independent factors to recognize the responses NOx produced using MINITAB 20.

$$\begin{aligned}
 NOx (ppm) = & +3186.59126 + 14.41204 blend (\%) \\
 & - 10.31663 FIP (bar) - 57.11164 EGR (\%) \\
 & - 26.45216 load (kg) - 0.037386 blend * FIP \\
 & + 0.385549 blend * EGR + 0.463453 blend * load \\
 & + 0.077110 FIP * EGR + 0.089357 FIP * load \\
 & - 0.631228 EGR * load + 0.219679 blend * blend \\
 & + 0.009187 FIP * FIP + 0.050365 EGR * EGR \\
 & + 2.86022 load * load
 \end{aligned}
 \tag{9}$$

The interaction impact of all control factors on NOx emission variation is depicted in Figure 9. Using 3-D response curves, Figure 9 (i) a and (i) b show the cumulative effect of blend ratio and EGR on NOx emission. As the quantity of biodiesel in the fuel mix grew, so did NOx emissions. In the presence of the chemically bound oxygen content in biodiesel (SOME), NOx generation rose and became significant, leading

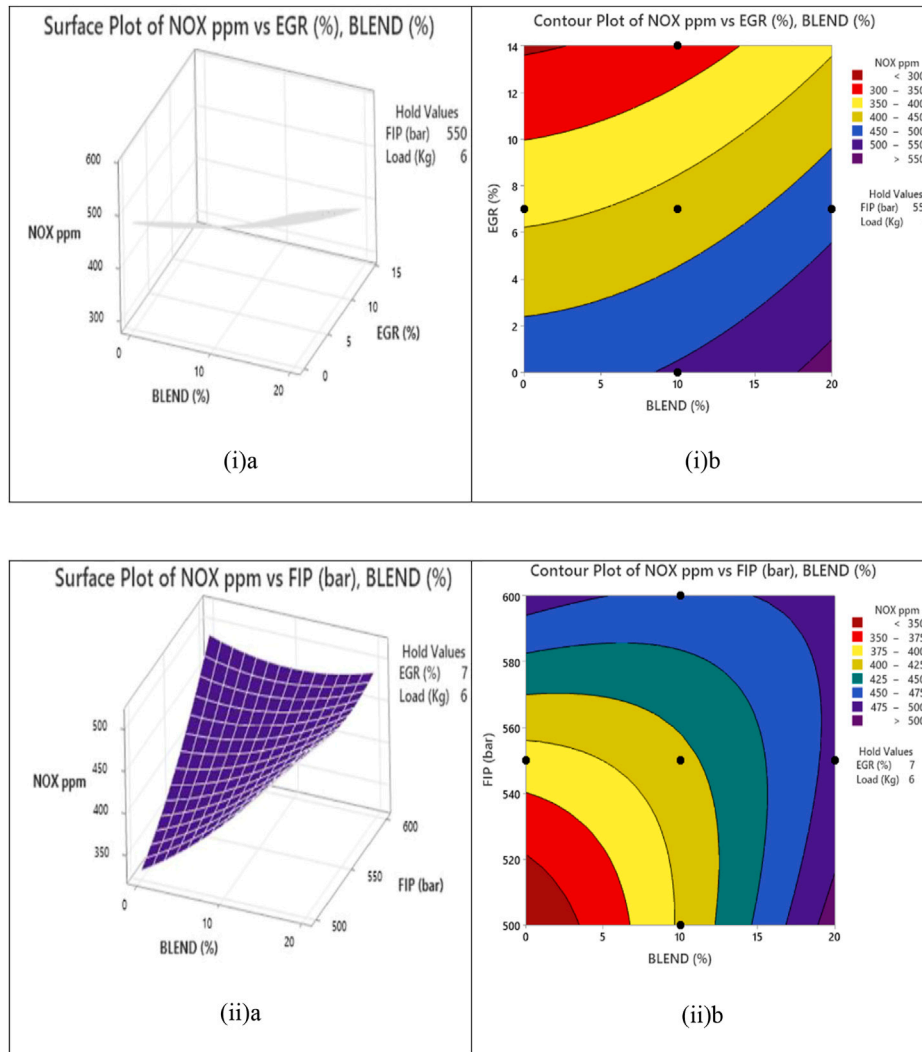


FIGURE 9
Effect of input factors on NO_x emission.

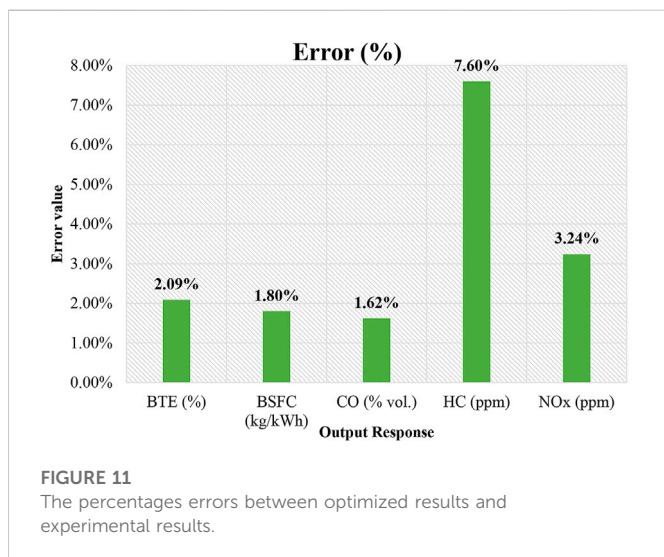
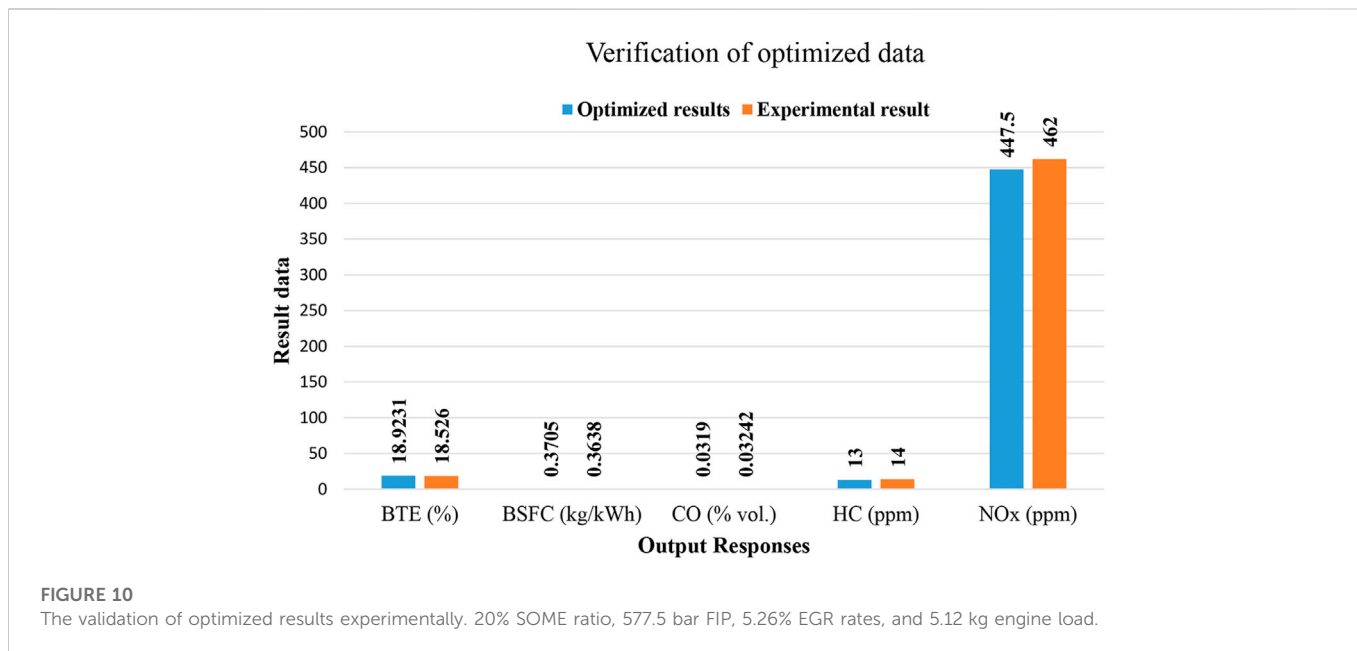
to higher levels of NO_x emissions than diesel fuel. The most important concern is the amount of NO_x emissions created by biodiesel combustion in engines. The primary purpose of the EGR technology in this study was to reduce NO_x emissions. When EGR is employed in CRDI engines, NO_x emissions are reduced. This was most likely due to the low temperature of the exhaust since the oxygen content in the cylinder's fresh air was decreasing. Because oxygen availability is lower at lower loads than at higher loads, NO_x generation at higher loads may be greater than at partial loads. Inefficient fuel combustion happens due to a shortage of oxygen in the combustion chamber, resulting in a low flame temperature, which inhibits the formation of NO_x. While higher EGR rates result in lower NO_x emissions, they also result in increased BSFC and lower BTE. [Bragadeshwaran et al. \(2019\)](#) also observed a reduction in NO_x emission with the employment of EGR on diesel engines fuelled with lemon peel oil and diesel blend.

The surface plot and contour surface in [Figure 9 \(ii\) a](#) and [\(ii\) b](#) show the impact of blend% and FIP on NO_x emission. Increasing injection pressure, as shown in this graph, enhanced NO_x emissions. The particle diameter reduced when the injection pressure was raised, and the

biodiesel–diesel fuel spray vaporized quickly. Liquid fuel, on the other hand, cannot penetrate very far into the combustion chamber. As a result, increased injection pressure initially results in quicker combustion rates and higher temperatures. As a result, NO_x concentrations begin to rise. [Mirhashemi and Sadrnia \(2020\)](#) found a similar trend with various biodiesel blends. The effects of blend % and load on NO_x emission fluctuation are depicted in [Figure 9 \(iii\) a](#) and [\(iii\) b](#). The NO_x emission is determined by the combustion chamber temperature, which is regulated by the applied load. As a result, increasing the load will always result in increased NO_x emissions. According to the study, NO_x emissions increased with increasing engine load for all of the fuels examined. Through a surface plot and contour surface, [Figure 9 \(iv\) a](#) and [\(iv\) b](#) demonstrates the influence of FIP and engine load on NO_x fluctuation.

5 Confirmation of the optimized results

The trials were repeated three times at the optimal parameters to confirm the optimized findings. The average of three measured outcomes was used to compute the actual responses. [Figure 10](#)



presents the average of the experimental values, and projected values, and Figure 11 shows the percentage errors of the corresponding output responses. Confirmation experiments were carried out on a diesel engine running on sesame biodiesel, with input parameters (20% SOME ratio, 577.5 bar FIP, 5.26% EGR rates, and 5.12 kg engine load) and performance and emission parameters (BTE, BSFC, CO, HC, and NOx) monitored. The RSM predictions were found to be within the allowed range with experimental findings when mean percentage errors were kept to a bare minimum. The verification findings showed that the models created were relatively accurate, with the percentages of prediction error in good agreement.

6 Conclusion

In this study, the effects of main operational factors including FIP, EGR, and load on the performance and emissions of a CRDI diesel engine were explored using biodiesel synthesized from sesame oil

blended with pure diesel to determine the best sesame biodiesel/diesel blends for CRDI engine performance and exhaust emissions to reduce BSFC, CO, HC, NOx and maximize the BTE. The Design of Experiments (DoE) based on response surface methodology (RSM) was extremely useful in designing the experiment, and the statistical analysis assisted in identifying the significant parameters that have the greatest influence on engine efficiency and emissions. To describe the correlations between performance and emission parameters, including input components SOME mix concentration, FIP, EGR, and engine load, a 2nd model was effectively created. The following conclusions can be made from this work.

- BTE was found to be maximum (28.188%) at process parameters i.e. blending of SOME 20%, 550 bar FIP, EGR 7%, and 12 kg engine load. At this configuration, the BSFC was also found to be minimum. The value of CO was obtained to be minimum (0.049%) at the no-load condition. The EGR has a great impact on NOx emissions. At 14% EGR rates, the emission of NOx reduces by 11%.
- The optimized NOx emission was obtained at 447.5 ppm at 20% SOME ratio, 577.5 bar FIP, 5.26% EGR rates, and 5.12 kg engine load.
- At 20% SOME ratio, 577.5 bar FIP, 5.26% EGR rates, and 5.12 kg engine load, high desirability of 79.6% was reached.
- This situation was deemed to have the best characteristics for the test engine, with 18.92% BTE, 0.3705 kg/kWh BSFC, and 0.03190% vol. CO, 13 ppm HC, and 447.5 ppm NOx emission.
- The ANOVA study revealed that the equivalent values of R^2 (96.35%, 87.54%, 91.57%, 95.87%, and 93.73% for BTE, BSFC, CO, HC, and NOx respectively) and adjusted R^2 in the current model suggest that the present proposed model could be effectively matched with the experimental outcomes.
- Under the 95% confidence level, all of the generated regression models for BTE, BSFC, CO, HC, and NOx were determined to be statistically significant.

Thus, by using the RSM technique, the number of experiments may be decreased, resulting in lower expenses and less time spent on future research. Furthermore, it is concluded that RSM is an effective optimization approach for CRDI engines operating under multi-objective optimization parameters. There is a future scope in the utilization of non-edible oil such as waste cooking oil. Other advantages of using waste cooking oil to generate biodiesel include waste product management and resource efficiency.

Data availability statement

The original contributions presented in the study are included in the article/Supplementary Material, further inquiries can be directed to the corresponding author.

Author contributions

MK: Methodology, conceptualization, validation, writing—original draft. RG: Writing—review and editing. NA: Investigation, writing—review and editing.

References

- Aljaafari, A., Fattah, I. M. R., Jahirul, M. I., Gu, Y., Mahlia, T. M. I., Islam, M. A., et al. (2022). Biodiesel emissions: A state-of-the-art review on health and environmental impacts. *Energies* 15 (18), 6854. doi:10.3390/en15186854
- Appavu, P., Madhavan, V. R., Venu, H., and Mariadoss, A. (2021). Effect of fuel additives and exhaust gas recirculation in biodiesel fuelled CI engine: A review. *Int. J. Ambient Energy* 42 (15), 1803–1809. doi:10.1080/01430750.2019.1614995
- Bhan, S., Gautam, R., and Singh, P. (2022). An experimental assessment of combustion, emissions, and performance behavior of diesel engine fuelled with New developed biofuel blend of two distinct waste cooking oils and metallic nano-particle (Al₂O₃). *Sci. Iran*. 0, 0. doi:10.24200/sci.2022.58882.5947
- Bhatia, S. K., Bhatia, R. K., Jeon, J. M., Pugazhendhi, A., Awasthi, M. K., Kumar, D., et al. (2021). An overview on advancements in biobased transesterification methods for biodiesel production: Oil resources, extraction, biocatalysts, and process intensification technologies. *Fuel* 285, 119117. doi:10.1016/j.fuel.2020.119117
- Bragadeshwaran, A., Kasianantham, N., Kaisan, M. U., Reddy, D. M. S., Aravind, K. M., Paul, N., et al. (2019). Influence of injection timing and exhaust gas recirculation (EGR) rate on lemon peel oil-fuelled CI engine. *Environ. Sci. Pollut. Res.* 26 (21), 21890–21904. doi:10.1007/s11356-019-05369-7
- Chaitanya, A. K., and Mohanty, D. K. (2022). Experimental investigation on the combustion, performance and emission characteristics of 1-pentanol blended waste plastic oil in a CRDI engine with EGR. *Energy* 256, 124574. doi:10.1016/j.energy.2022.124574
- Chelladurai, S. J. S., Murugan, K., Ray, A. P., Upadhyaya, M., Narasimharaj, V., and Gnanasekaran, S. (2021). Optimization of process parameters using response surface methodology: A review. *Mater. Today Proc.* 37, 1301–1304. doi:10.1016/j.matpr.2020.06.466
- Devaraj, A., Devarajan, Y., and Vinoth, K. I. (2021). Effect of di-ethyl-ether on biodiesel fuelled diesel engine. *Int. J. Ambient Energy* 42 (5), 495–499. doi:10.1080/01430750.2018.1557546
- Ganesan, S., Reddy, O. Y., Reddy, K. J., and Rahul, P. (2021). WITHDRAWN: Exploration of performance and emissions characteristics of Gossypium arboreum biodiesel on diesel engine. *Mater. Today Proc.* doi:10.1016/j.matpr.2021.02.720
- Govindasamy, P., Antony, A. G., Rajaguru, K., and Saravanan, K. (2019). Experimental investigation of the effect of compression ratio in a direct injection diesel engine fuelled with spirulina algae biodiesel. *J. Appl. Fluid Mech.* 11, 107–114. doi:10.36884/jafm.11.SI.29426
- Jayabal, R., Thangavelu, L., and Subramani, S. (2020). Combined effect of oxygenated additives, injection timing and EGR on combustion, performance and emission characteristics of a CRDI diesel engine powered by sapota biodiesel/diesel blends. *Fuel* 276, 118020. doi:10.1016/j.fuel.2020.118020
- Khanjani, A., and Sobati, M. A. (2021). Performance and emission of a diesel engine using different water/waste fish oil (WFO) biodiesel/diesel emulsion fuels: Optimization of fuel formulation via response surface methodology (RSM). *Fuel (Lond)*. 288, 119662. doi:10.1016/j.fuel.2020.119662
- Kim, H. Y., Ge, J. C., and Choi, N. J. (2019). Effects of fuel injection pressure on combustion and emission characteristics under low speed conditions in a diesel engine fuelled with palm oil biodiesel. *Energies* 12 (17), 3264. doi:10.3390/en12173264
- Kumar, M., Ansari, N. A., Sharma, A., Singh, V. K., Gautam, R., and Singh, Y. (2021b). Prediction of an optimum engine response based on different input parameters on common rail direct injection diesel engine: A response surface methodology approach. *Sci. Iran* 28 (6), 3181–3200. doi:10.24200/SCI.2021.56745.4885
- Kumar, M., Singh, V. K., Sharma, A., Ansari, N. A., Gautam, R., and Singh, Y. (2021a). Effect of fuel injection pressure and EGR techniques on various engine performance and emission characteristics on a CRDI diesel engine when run with linseed oil methyl ester. *Energy and Environ.* 33, 41–63. doi:10.1177/0958305X20983477
- Mehra, K. S., and Pant, G. (2021). Production of biofuel from sesame oil and its characterization as an alternative fuel for diesel engine IOP conference series: Materials science and engineering. *IOP Publ.* 1116 (1), 012076. doi:10.1088/1757-899x/1116/1/012076
- Mirhashemi, F. S., and Sadriani, H. (2020). NO_x emissions of compression ignition engines fuelled with various biodiesel blends: A review. *J. Energy Inst.* 93 (1), 129–151. doi:10.1016/j.joei.2019.04.003
- Mujtaba, M. A., Cho, H. M., Masjuki, H. H., Kalam, M. A., Farooq, M., Soudagar, M. E. M., et al. (2021). Effect of alcoholic and nano-particles additives on tribological properties of diesel-palm-sesame-biodiesel blends. *Energy Rep.* 7, 1162–1171. doi:10.1016/j.egy.2020.12.009
- Mutuk, T., and Mesci, B. (2014). Analysis of mechanical properties of cement containing boron waste and rice husk ash using full factorial design. *J. Clean. Prod.* 69, 128–132. doi:10.1016/j.jclepro.2014.01.051
- Nanthagopal, K., Ashok, B., Kishna, R. S., Srinath, R., Kumar, M. P., and Karthickeyan, V. (2020). Experimental investigation on engine parameters variation in common rail direct injection engine fuelled with biodiesel. *Clean Technol. Environ. Policy* 22 (2), 459–479. doi:10.1007/s10098-019-01796-9
- Oni, B. A., and Oluwatosin, D. (2020). Emission characteristics and performance of neem seed (*Azadirachta indica*) and Camelina (*Camelina sativa*) based biodiesel in diesel engine. *Renew. Energy* 149, 725–734. doi:10.1016/j.renene.2019.12.012
- Pali, H. S., Sharma, A., Kumar, N., and Singh, Y. (2021). Biodiesel yield and properties optimization from Kusum oil by RSM. *Fuel* 291, 120218. doi:10.1016/j.fuel.2021.120218
- Pamnani, R., Vasudevan, M., Vasantharaja, P., and Jayakumar, T. (2017). Optimization of A-GTAW welding parameters for naval steel (DMR 249 A) by design of experiments approach. *Proc. Institution Mech. Eng. Part L J. Mater. Des. Appl.* 231 (3), 320–331. doi:10.1177/1464420715596455
- Pavan, P., Bhaskar, K., and Sekar, S. (2021). Effect of split injection and injection pressure on CRDI engine fuelled with POME-diesel blend. *Fuel* 292, 120242. doi:10.1016/j.fuel.2021.120242

Acknowledgments

The author(s) would like to express gratitude to the academic members of the Mechanical Engineering Department at Delhi Technological University in Delhi, India, for making this experiment possible by providing the necessary equipments and machines.

Conflict of interest

The authors declare that the research was conducted in the absence of any commercial or financial relationships that could be construed as a potential conflict of interest.

Publisher's note

All claims expressed in this article are solely those of the authors and do not necessarily represent those of their affiliated organizations, or those of the publisher, the editors and the reviewers. Any product that may be evaluated in this article, or claim that may be made by its manufacturer, is not guaranteed or endorsed by the publisher.

- Pereira, L. M. S., Milan, T. M., and Tapia-Blácido, D. R. (2021). Using response surface methodology (RSM) to optimize 2G bioethanol production: A review. *Biomass Bioenergy* 151, 106166. doi:10.1016/j.biombioe.2021.106166
- Ramachander, J., and Gugulothu, S. K. (2022). Performance, combustion, and emission characteristics of a common rail direct injection diesel engine fueled by diesel/n-amy alcohol blends with exhaust gas recirculation technique. *J. Energy Resour. Technol.* 144 (3). doi:10.1115/1.4052977
- Rathore, Y., Ramchandani, D., and Pandey, R. K. (2019). Experimental investigation of performance characteristics of compression-ignition engine with biodiesel blends of Jatropa oil and coconut oil at fixed compression ratio. *Heliyon* 5 (11), e02717. doi:10.1016/j.heliyon.2019.e02717
- Rejeb, O., Yousef, M. S., Ghenai, C., Hassan, H., and Bettayeb, M. (2021). Investigation of a solar still behaviour using response surface methodology. *Case Stud. Therm. Eng.* 24, 100816. doi:10.1016/j.csite.2020.100816
- Samet, U. S. L. U., and Yeşilyurt, M. K. (2020). Improving the running conditions of diesel engine with grape seed oil additives by response surface design. *Int. J. Automot. Sci. Technol.* 4 (3), 185–192. doi:10.30939/ijastech.770058
- Sathyanarayanan, S., Suresh, S., Uslu, S., Shivaranjani, R. S., Chandramohan, V. P., and Simsek, S. (2022). Optimization of gasoline engine emission parameters employing commercial and sucrolite-catalyst coated converter using response surface methodology. *Int. J. Environ. Sci. Technol.*, 1–14. doi:10.1007/s13762-022-03968-5
- Sayyed, S., Das, R. K., and Kulkarni, K. (2022). Experimental investigation for evaluating the performance and emission characteristics of DIC engine fueled with dual biodiesel-diesel blends of Jatropa, Karanja, Mahua, and Neem. *Energy* 238, 121787. doi:10.1016/j.energy.2021.121787
- Seeniappan, K., Venkatesan, B., Krishnan, N. N., Kandhasamy, T., Arunachalam, S., Seeta, R. K., et al. (2022). A comparative assessment of performance and emission characteristics of a DI diesel engine fuelled with ternary blends of two higher alcohols with lemongrass oil biodiesel and diesel fuel. *Energy and Environ.* 33 (6), 1134–1159. doi:10.1177/0958305X211051323
- Sharif, S. K., Nageswara Rao, B., and Jagadish, D. (2020). Comparative performance and emission studies of the CI engine with Nodularia Spumigena microalgae biodiesel versus different vegetable oil derived biodiesel. *SN Appl. Sci.* 2 (5), 858–859. doi:10.1007/s42452-020-2697-0
- Sharma, A., Pali, H. S., Kumar, M., Singh, N. K., Rahim, E. A., Singh, Y., et al. (2022). Effect of α -aluminium oxide nano additives with Sal biodiesel blend as a potential alternative fuel for existing DI diesel engine. *Energy and Environ.*, 0958305X22113325. doi:10.1177/0958305X221133257
- Shrivastava, P., and Verma, T. N. (2020). Effect of fuel injection pressure on the characteristics of CI engine fuelled with biodiesel from Roselle oil. *Fuel* 265, 117005. doi:10.1016/j.fuel.2019.117005
- Shrivastava, P., Verma, T. N., and Pugazhendhi, A. (2019). An experimental evaluation of engine performance and emission characteristics of CI engine operated with Roselle and Karanja biodiesel. *Fuel* 254, 115652. doi:10.1016/j.fuel.2019.115652
- Simsek, S., Uslu, S., and Simsek, H. (2022). Response surface methodology-based parameter optimization of single-cylinder diesel engine fueled with graphene oxide dosed sesame oil/diesel fuel blend. *Energy AI* 10, 100200. doi:10.1016/j.egyai.2022.100200
- Singh, D. K., and Tirkey, J. V. (2022). Performance optimization through response surface methodology of an integrated coal gasification and CI Engine fuelled with diesel and low-grade coal-based producer gas. *Energy* 238, 121982. doi:10.1016/j.energy.2021.121982
- Singh, T. S., and Verma, T. N. (2019). Biodiesel production from Momordica charantia (L.): Extraction and engine characteristics. *Energy* 189, 116198. doi:10.1016/j.energy.2019.116198
- Srinidhi, C., Madhusudhan, A., Channapattana, S. V., Gawali, S. V., and Aithal, K. (2021). RSM based parameter optimization of CI engine fuelled with nickel oxide dosed Azadirachta indica methyl ester. *Energy* 234, 121282. doi:10.1016/j.energy.2021.121282
- Uslu, S., Yeşilyurt, M., and Yaman, H. (2022). Impact prediction model of acetone at various ignition advance by artificial neural network and response surface methodology techniques for spark ignition engine. *Sci. Technol. Energy Transition (STET)* 77, 7. doi:10.2516/stet/2022010
- Venkatesan, V., Nallusamy, N., and Nagapandiselvi, P. (2021). Performance and emission analysis on the effect of exhaust gas recirculation in a tractor diesel engine using pine oil and soapnut oil methyl ester. *Fuel* 290, 120077. doi:10.1016/j.fuel.2020.120077
- Yadav, P. S., and Gautam, R. (2022). Numerical and experimental analysis on spray characteristics of biodiesel (waste cooking oil) using pressure swirl atomizer. *Environ. Prog. Sustain. Energy* 41 (3), e13761. doi:10.1002/ep.13761
- Yesilyurt, M. K. (2020). The examination of a compression-ignition engine powered by peanut oil biodiesel and diesel fuel in terms of energetic and exergetic performance parameters. *Fuel* 278, 118319. doi:10.1016/j.fuel.2020.118319
- Yesilyurt, M. K., Uslu, S., and Yaman, H. (2022). Modeling of a port fuel injection spark-ignition engine with different compression ratios using methanol blends with the response surface methodology. *Proc. Institution Mech. Eng. Part E J. Process Mech. Eng.*, 095440892211123. doi:10.1177/09544089221112373

Nomenclature

ASTM American society for testing and materials

ANOVA Analysis of variance

BTE Brake thermal efficiency

BSFC Brake specific fuel consumption

CCD Central composite design

CRDI Common rail direct injection

CO Carbon monoxide

CN Cetane number

CR Compression ratio

CV Calorific value

DoE Design of expert

EGR Exhausts gas recirculation

EGT Exhaust gas temperature

FIP Fuel injection pressure

HC Hydrocarbon

IT Injection timing

ID Ignition delay

KOH Potassium hydroxide

NO_x Nitrogen oxide

RSM Response surface methodology

SOME Sesame oil methyl ester

VCR Variable compression ratio.